



**HAL**  
open science

# Complete Dynamic Phase Diagram of a Supramolecular Polymer

Nikolaos Burger, Gaelle Pembouong, Laurent Bouteiller, Dimitris Vlassopoulos, Benoit Loppinet

► **To cite this version:**

Nikolaos Burger, Gaelle Pembouong, Laurent Bouteiller, Dimitris Vlassopoulos, Benoit Loppinet. Complete Dynamic Phase Diagram of a Supramolecular Polymer. *Macromolecules*, 2022, 55 (7), pp.2609-2614. 10.1021/acs.macromol.1c02508 . hal-03857181

**HAL Id: hal-03857181**

**<https://hal.science/hal-03857181>**

Submitted on 17 Nov 2022

**HAL** is a multi-disciplinary open access archive for the deposit and dissemination of scientific research documents, whether they are published or not. The documents may come from teaching and research institutions in France or abroad, or from public or private research centers.

L'archive ouverte pluridisciplinaire **HAL**, est destinée au dépôt et à la diffusion de documents scientifiques de niveau recherche, publiés ou non, émanant des établissements d'enseignement et de recherche français ou étrangers, des laboratoires publics ou privés.

# Complete dynamic phase diagram of a supramolecular polymer

Nikolaos A. Burger<sup>1,2</sup>, Gaëlle Pembouong<sup>3</sup>, Laurent Bouteiller<sup>3</sup>, Dimitris Vlassopoulos<sup>1,2</sup>, Benoit Loppinet<sup>1</sup>

1 Foundation for Research & Technology Hellas (FORTH), Institute for Electronic Structure & Laser, Heraklion 70013, Greece

2 University of Crete, Department of Materials Science & Technology, Heraklion 70013, Greece

3 Sorbonne Université, CNRS, IPCM, Equipe Chimie des Polymères, 75005 Paris, France

Corresponding author: B. Loppinet ([benoit@iesl.forth.gr](mailto:benoit@iesl.forth.gr))

## Abstract

We revisit the equilibrium phase diagram of the much studied model supramolecular polymer, 2,4-bis(2-ethylhexylureido)toluene (EHUT) in non-polar solvents, which had previously been studied at atmospheric pressure, and provide unambiguous evidence of a much richer behavior, characterized by four distinct regimes. Typically, two types of self-assembled structures are formed: tubes (filaments) at higher (lower) concentrations and lower (higher) temperatures, respectively. The tube structure forms viscoelastic solutions that had been characterized by rheology, however without detailed analysis of the experimental signals. Here, we combine rheology and microrheology to establish the complete dynamic phase diagram of EHUT in dodecane. It still comprises two structures, tubes and filaments, with the transition temperature being almost constant over the examined wide concentration range, as confirmed with the help of complementary differential scanning calorimetry measurements. The tubes are found to exist in three dynamic states with increasing concentration, unentangled, partially entangled and well-entangled, which are separated by iso-length lines. We present criteria for unambiguously identifying these phases and discuss their distinct concentration and temperature dependencies. The new, complete phase diagram may serve as guide for investigating other supramolecular polymers with tunable rheology and, more importantly, providing insights toward a universal description of one-dimensional self-assembled structures by linking this class of materials with the classic wormlike surfactant micelles, for which the partially and well-entangled regimes were recently elucidated.

## Introduction

Supramolecular polymers are self-assemblies of molecules (monomers) with directional attractions forming non-covalent bonds. Interactions may be such that the assemblies are in dynamic equilibrium through break and reform mechanisms, forming living polymers. This class of macromolecules has attracted a lot of attentions with significant efforts focused on tailoring the self-assembly process (i.e, effective non-covalent polymerization) by selecting appropriate motifs and by exploiting their resulting widespread practical applicability.<sup>1-4</sup> The dynamic nature of the supramolecular polymers through break and reform mechanism is essential in defining and controlling their bulk properties and in particular their rheology.<sup>5-7</sup> The strength and range of the

interaction dictates the equilibrium length distribution of the assembly and its dynamics. Strong binding leads to low breaking probabilities and properties similar to conventional (covalently bonded) polymers. Weak binding yields relatively short self-assemblies. The difference is easily noticeable in the linear viscoelastic response since sufficiently long supramolecular polymers can entangle and form transient networks, whereas their short counterparts form viscous solutions.

Hydrogen bonding motifs lead to reversible associations with high strength and the resulting supramolecular polymers are ubiquitous in applications for the research purposes.<sup>8</sup> In this work we examine the properties of an archetype supramolecular polymer based on the bis-urea monomer, 2,4-bis(2-ethylhexylureido)toluene (EHUT).<sup>9</sup> Under atmospheric pressure, at large enough concentrations in non-polar solvents such as toluene<sup>10</sup>, cyclohexane<sup>11</sup> or dodecane<sup>12-14</sup> EHUT self-assembles into long supramolecular polymers, with two distinct conformations, tubes and filaments at lower and higher temperatures, respectively.<sup>15-17</sup> The two forms, tubes and filaments, are characterized by a different molecular arrangement with a larger cross section and mass per unit length for the tube phase schematically depicted in Figure 1. They also exhibit distinct rheological properties. We have recently employed passive microrheology to obtain the linear viscoelastic (LVE) spectrum over a broad frequency range at different temperatures and pressures and shown that high pressures promote tube formation.<sup>18</sup>

So far the EHUT rheology has been discussed in terms of viscous liquid (filaments) and viscoelastic entangled (tubes) solutions, in harmony with the established picture dictating the behavior of worm-like surfactant micelles, WLMs, which served as the prototype supramolecular polymer system (albeit with distinct differences from hydrogen bonded assemblies, such as their ability to form spherical micelles as well, exhibit long-range order and possessing properties depending on charge interactions). **But WLMs also exist in intermediate rheological states, such as un-entangled and partially (or weakly) entangled as realized 20 years ago.**<sup>19</sup> More recently<sup>20</sup> the partially entangled regime was attributed through simulations to shorter length of the order of the entanglement length. Motivated by this development, we address here the challenge of establishing the complete phase diagram of EHUT in non-polar solvents, encompassing tubes and filaments, and in particular we explore different dynamic states and their transitions, which have not been revealed so far. In this regard, it is important to note that the available rheological data with EHUT are limited to the frequency range accessible in standard rheometry, while application of time-temperature superposition is questionable and certainly not widely applicable because of the potential temperature-induced changes in the strength of interactions.<sup>21</sup> To overcome this problem we combine conventional rheology with microrheology at a given temperature. With the addition of

complementary dynamic light scattering (DLS) and differential scanning calorimetry (DSC) experiments, we accomplish a careful and systematic rheological characterization of EHUT in dodecane, covering a broad range of concentrations and temperatures. We establish its complete dynamic phase diagram, putting into evidence the tube to filament thermodynamic transition and the gradual evolution of the LVE properties. In particular, we identify three different LVE regimes in the lower-temperature tube phase, unentangled (UE), partially entangled (PE) and well-entangled (WE). We present quantitative criteria to distinguish them and discuss the implications of this rich behavior to materials bulk properties and modeling.

## Experimental Section

### Materials and Methods

The synthesis of EHUT was achieved by reacting racemic 2-ethylhexylamine with 2,4-toluene diisocyanate.<sup>9</sup> Dodecane (99.7 % pure) was obtained from Sigma Aldrich and used as received. The solutions were prepared in ambient conditions. . EHUT powder was added to the filtered solvent at room temperature and the mixture was stirred for at least 48 hours at 80° C in a sealed vial. Solutions were left unstirred for 24 h and transferred with in NMR tube for light scattering and microrheology measurements Dodecane was used in ambient conditions with no effort to control water amount. Presence of traces amount of water is known to strongly affect the properties of the EHUT solutions, and in particular the linear viscoelasticity and the viscosities.<sup>13</sup> In this work we assumed steady state conditions. No drift that would be associated with changing amount of water were noticed. Sterically stabilized PMMA hard sphere particles (130 nm radius, grafted with short layer of poly(hydrostearic-acid) for stabilization) used as scattering probes were dispersed in pre-prepared EHUT-dodecane solutions.<sup>22</sup> Volume fraction (0.01%) ensured that scattering is dominated by the non-interacting probes and remained single scattering.

DSC thermograms were measured using a N-DSCIII instrument from TA Instruments at a scan rate of 1°C/min. The reference cell was filled with dodecane and the sample cell (0.3 mL) with EHUT solution. The capillary cells were not capped, and a constant pressure of 5x10<sup>5</sup> Pa was applied. The transition temperature and enthalpy were measured from the second heating scan. The lower concentrations solutions (between 0.1 and 0.8 g/L) viscosity were measured at 25 ±0.1 °C with a Lovis 2000 rolling-ball microviscometer (Anton Paar, Austria). High concentrations at 8 and 12g/L and T ≤ 65 °C were probed using an Anton-Paar MCR-501 rheometer, operating in the strain-controlled mode, equipped with a Peltier unit for temperature control (±0.1°C at the bottom plate),

and a stainless steel cone plate geometry (25mm, cone angle 4°)-and-plate geometry and homemade cover to limit solvent contact with air. Samples were loaded at 20°C under ambient humidity (RH~44%). Measurements were repeated (at least) twice to ensure reproducibility. Dynamic and static light scattering experiments (DLS and SLS, respectively), were performed with two goniometer/correlator setup, a ALV 5000 and a home built goniometer setup used at 90° angle with a controlled temperature cell ( $T_{\max} > 150$  °C). Both used single mode CW laser ( $\lambda = 532$  nm) as light source (Fig. S1). Temperature dependence of the SLS and DLS could be used to identify the different phases. Single scattering DLS passive microrheology measurements were performed with the same setups. Sterically stabilized PMMA hard sphere particles (130 nm radius, grafted with short layer of poly(hydrostearic-acid) for stabilization) scattering probes were dispersed in pre-prepared EHUT-dodecane solutions.<sup>22</sup> Volume fraction (0.01%) ensured that scattering is dominated by the non-interacting probes and remained single scattering. The measured intensity autocorrelation function  $g_2(q, t)$  was analyzed in terms of the probe's mean square displacement (MSD), yielding  $3q^2 \langle \Delta r^2(t) \rangle = \log(g_2(t)/f^*)$ , where  $q$  is the scattering wave vector and  $f^*$  an experimental factor, in our case  $f^* = 1$ . Within the microrheology conditions (large enough probe, limited interaction between probe and the sample), MSD provides a measure of the macroscopic creep compliance  $J(t)$ .<sup>23-25</sup> The latter was converted to storage ( $G'(\omega)$ ) and loss ( $G''(\omega)$ ) moduli by means of the NLReg software, based on a generalization of the Tikhonov regularization method.<sup>26</sup> The different steps are illustrated in SI (fig S4).

Viscosities were extracted from LVE measurements in different ways depending on the viscoelastic spectrum. In viscous solutions, it was directly obtained from the single exponential decay field correlation function (or from the equivalent mean square displacement) assuming diffusion and using Stokes Einstein equation. In the case of viscoelastic solution, it was obtained through extrapolation of the Newtonian plateau from the dynamic viscosity at low frequency (or equivalently from creep compliance at long time) as depicted in fig. S5.

## Results and Discussion

The tube-to-filament transition has been probed by DSC in a range of non-polar solvents<sup>16</sup>, however, only one concentration was investigated in dodecane.<sup>27</sup> Figure 1 shows DSC traces measured at different concentrations. A clear peak marking the transition is unambiguously discerned at all concentrations. The extracted transition temperature and the enthalpy are depicted in the inset as a function of concentration. Both are shown to be nearly independent of concentration with less than 1K variation of the temperature over the entire range investigated. The enthalpy is ~3.5kJ/mol only

weakly dependent on the concentration in agreement with studies in toluene.<sup>10</sup> The DSC transition is accompanied by an abrupt change of scattering intensity, as shown in the SI<sup>18</sup>, in figure S3, and of viscosity as discussed below.

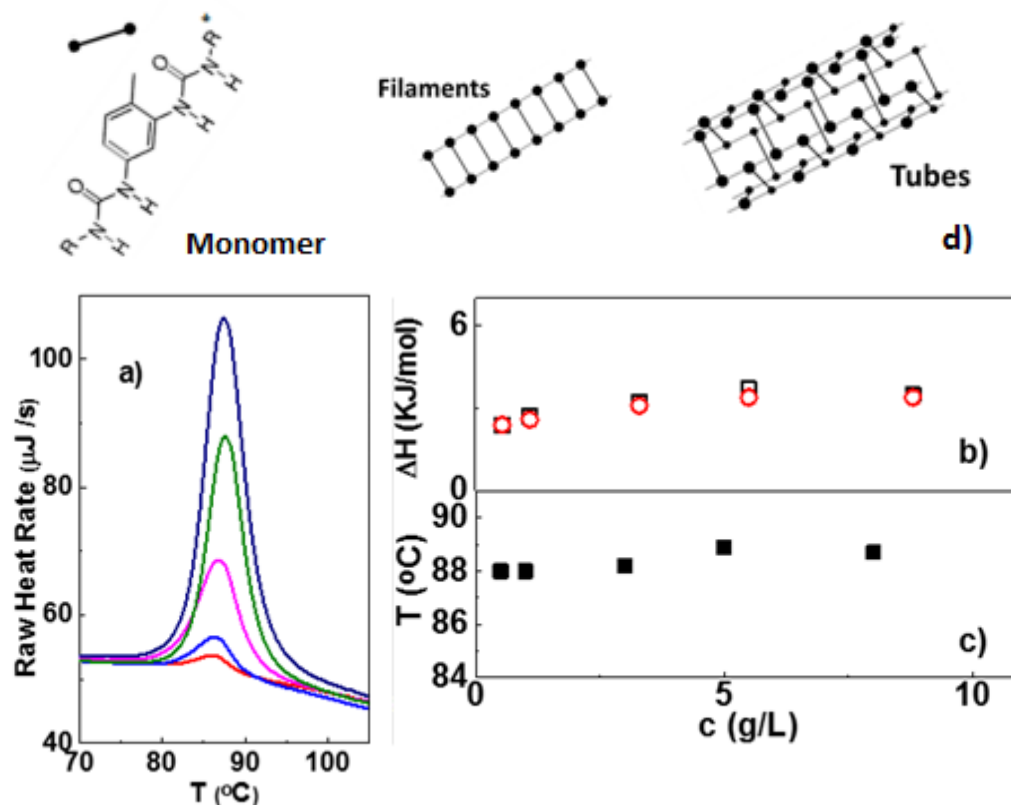


**Figure 1:** a) DSC traces during heating for different EHUT concentrations (0.5, 1, 3, 5, 8 g/L from bottom to top). b) Enthalpy during heating (red squares) and cooling (black squares) and c) tube to filament transition temperature as a function of concentration. d) Schematic illustration of three possible configurations from left to right: single EHUT molecules, filament structure and tubular structure. **Black dots indicate the hydrogen bond between EHUT molecules.**

The occurrence of the two different structures, tubes and filaments, and the associated quasi-first order transition have been discussed in the context of directed interactions and the local packing of solvent molecules, i.e., their size relative to the tube diameter.<sup>16, 17, 28</sup>

The evolution of the measured microrheology-based LVE spectra at different EHUT temperatures and concentrations is depicted in Fig. 2 (and Fig S6). The temperature dependence of the solvent viscosity ( $\eta_0(T)$  measured through microrheology) is accounted for **in the x-axis**, so the observed effects **directly** reveal changes associated to EHUT self-assemblies. The speed-up of dynamics as the temperature increases is apparent at all concentrations. The qualitative changes can be discerned in Figs. 2a and 2b for concentrations of 3 g/L and 3.6 g/L, respectively.

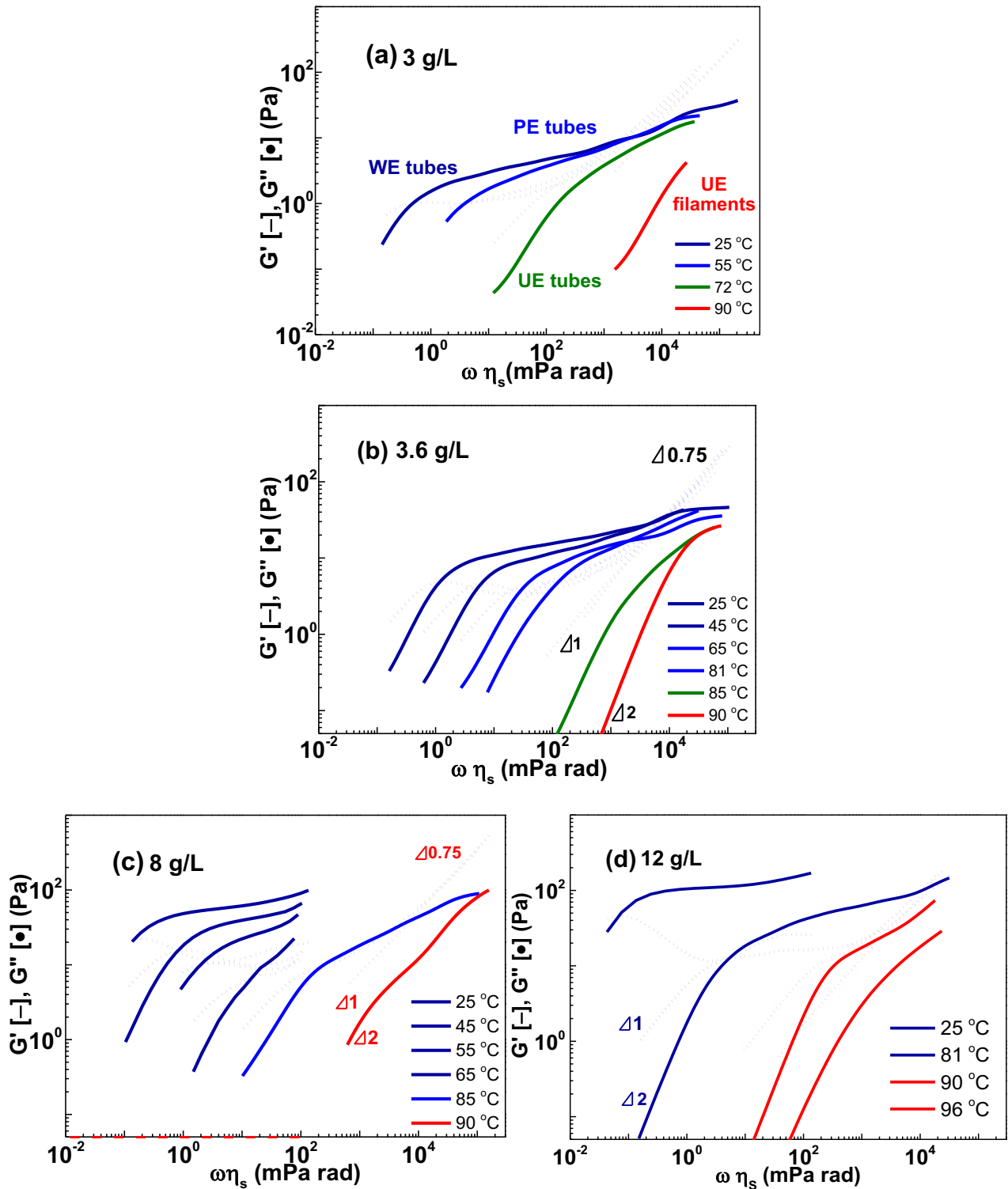


**Figure 2:** Temperature evolution of LVE spectra (storage modulus -  $G'$  solid lines, loss modulus -  $G''$  dots) of EHUT- dodecane solution for different concentrations at a) 3 b) 3.6 c) 8 d) 12 g/L. WE, PE and UE stand for well-entangled, partially entangled and unentangled respectively; Colors: tube phases: deep blue for WE, light blue for PE, green for UE, filament phase red for UE. Rheometer data 8g/L 25°C to 65°C, 12g/L 25°C), all the rest is microrheology.

At lower temperatures, a well-pronounced maximum in the loss modulus  $G''$  is observed. It coincides with the cross-over between  $G'$  and  $G''$ , as expected for Maxwellian response with one terminal time and observed in living wormlike micelles.<sup>19,20,29</sup> In this situation,  $G'$  exhibits an unambiguous plateau which extends over more than two decades in frequency. As the temperature increases, the low-frequency moduli cross-over is still detected, along with a  $G'$  plateau (at higher frequencies) where  $G' > G''$ . However the peak is weaker and the plateau turns into a weak power-law regime, more pronounced at higher temperatures, while the terminal  $G''$  maximum broadens until eventually it disappears. These features signify the transition from the well-entangled regime to a partially entangled regime. Such a behavior was recently identified for surfactant WLMs.<sup>20</sup> At even higher temperatures,  $G'' > G'$  over the entire frequency range, with a frequency dependence ranging from terminal **flow at low frequency** to **power law regime** typical of semiflexible chains at larger frequency, signifying the rheological response of unentangled supramolecular polymers (fig. S8). Such predominantly viscous response was probed both in the tube ( $T < 89^\circ\text{C}$ ) and the filament ( $T > 89^\circ\text{C}$ ) phases. However, the latter never exhibited entangled LVE spectrum in the explored concentration regime. We therefore identify three LVE regimes in the tube phase of EHUT-dodecane, well-entangled (WE), partially entangled (PE) and unentangled (UE).

The existence of an intermediate partially entangled regime is to be expected in systems where the average length becomes comparable to the entanglement length  $L_e$ . The transition from unentangled Rouse to well-entangled linear polymer chains is a **gradual one**, marked by an **intermediate** weakly entangled regime (typically with  $Z < 10$  entanglements).<sup>30</sup> **Moreover the specific polydispersity of the supramolecular living polymer is expected to broaden this domain.**<sup>34</sup> An alternative indicator of the occurrence of well-entangled tube phase is the value of the ratio of high to low frequency cross-over of  $G'$  and  $G''$ . It was reported to exceed a value of 300 in the well-entangled regime for WLM<sup>20</sup>; **The agreement between the two methods is confirmed here as shown in Fig. 3 reporting the ratio of the high to the low frequency for the different concentration and temperature as a function of concentration. The well entangled solutions are situated above the dotted line at  $\omega_2 \setminus \omega_1 = 350$ .**

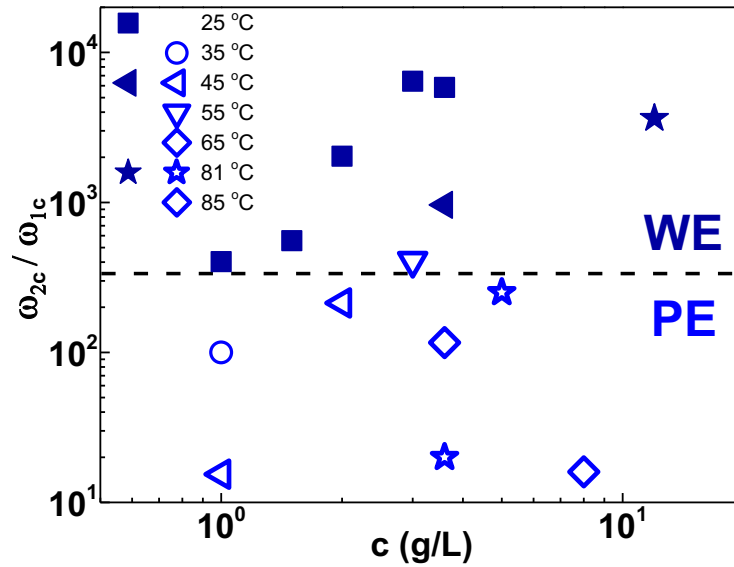


**Figure 3:** Ratio of high to low frequency crossovers of shear modulus as a function of EHUT concentration for different temperatures. Open symbols correspond to partially entangled solutions, filled to well entangled. The black dashed line (ratio = 350) separates the partially to well entangled regimes.

The resulting dynamic phase diagram in the temperature-concentration plane is shown in Fig. 4, showing the filament phase at high temperature ( $T > 89^\circ\text{C}$ ) and the three rheological states of the tube phase at lower temperatures. At the lower temperatures, the unentangled and partially entangled regimes seem to converge to a constant concentration  $c \sim 1$  g/L, independent of temperature. Lines that separate the different tube states represent the temperature dependence of the concentration threshold for UE to PE and for PE to WE. If plotted in an activation type representation ( $\ln c$  vs  $1/T$  as shown in SI fig S10) the lines that separate the rheological states are two parallel straight lines, separated by a factor of 4 in concentration. The corresponding equations are  $\frac{E_a}{k_B T} = -\ln(K_l c_l)$  where  $c_l$  is the value of  $c$  at the limit and  $K_l$  and  $E_a$  are parameters with values  $E_a = 40 \text{ kJ/mol}$  (or  $16 k_B T$ ) and  $K_l = 280 \times 10^{-9}$  and  $80 \times 10^{-9}$  L/g for UE-PE and PE-WE limit respectively. The resulting lines are shown by the dashed lines in Fig. 3. The meaning of this can be discussed in the context of Cates living polymer theory. Based on polymer solutions rheology, the thresholds are expected to be located at specific  $c/c^*$  values.

The effect of temperature and concentration can be evaluated in the context of the living polymer model of Cates, largely used in WLM and also in EHUT previous studies. The average aggregation number (degree of polymerization of the supramolecular chains) break and reform  $\bar{N}$ . Assuming the break and reform rates independent of chain length, the chains adopt at any time a well-defined

distribution with an average  $\bar{N}$  that depends on concentration and temperature as  $\bar{N} \sim \sqrt{c} e^{\frac{E}{2k_B T}}$ ,  $k_B$  Boltzmann's constant, and  $E$  the activation energy associated with end formation, which is considered to be independent of concentration and temperature.<sup>6</sup> The average contour length  $L = \bar{N}b$  where  $b$  is a microscopic length. Defining the overlap concentration  $c^* = \bar{N} \cdot m_o / R^3$  with  $R$  the characteristic average radius,  $m_o$  the monomer mass. For theta solvent where  $R \sim \bar{N}^{1/2}$  we get  $\frac{c}{c^*} \sim c \bar{N}^{\frac{1}{2}} \sim c^{1.25} e^{\frac{E}{4k_B T}}$ . Therefore  $c/c^*$  grows faster than  $c$  (at constant  $T$ ), as increase in monomer concentration  $c$  also induces a decrease of  $c^*$  through an increase of  $\bar{N}$ .

The two delimiting lines are about a factor of  $\sim 4$  apart in concentration, which corresponds to a factor of 2 in length and a factor of 6 in  $c/c^*$ . The numbers is compatible with the results of WLM rheology where the two domains were reported (at constant concentration) at 2 and 5  $L_e$ <sup>20</sup> and also in good agreement with the results observed in polymer solutions.

If threshold lines are at constant  $c/c^*$ , their evolution should then follow  $c^{1.25} e^{\frac{E}{4k_B T}} = cste$  or  $\frac{E}{(4 \cdot 1.25) k_B T} = \ln(cste/c)$  so that the apparent activation energy  $E_a = E/5$ .  $E_a$  therefore provides an estimate of the break-recombination or cap energy  $E = 200 kJ/mol$  (or 90  $k_B T$ ). This value of  $E$  is reasonable but a factor of 2 of previously reported number.<sup>14</sup> The rather large value implies large aggregation number. The  $K_l$  values also reflects the length of the assembly at the specific concentration and temperature.

The UE to PE threshold and the associated sharp increase of viscosity is often incorrectly taken as a measure of the overlap concentration  $c^*$ . It should rather be assigned to the onset of entanglement, located at larger concentration than the overlap concentration (typically order of 5 to 10  $c^*$ ).<sup>29</sup>

The specific polydispersity of living polymer is expected to have an impact on the evolution of the LVE, making the intermediate state of unentangled at  $c > c^*$  larger in  $c$ -range.

Based on polymer and WLM rheology, at a given concentration, PE solutions are expected when the average length is of the order of few entanglement lengths, typically between 2 and 5  $L_e$ .<sup>20</sup>

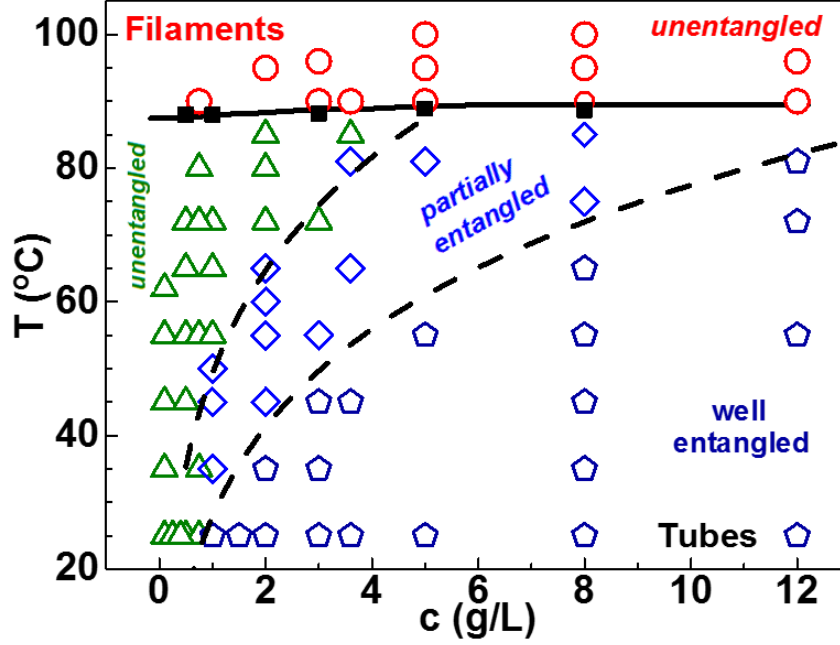


**Figure 4:** Dynamic phase diagram of EHUT solution in dodecane, presented in the temperature-concentration plane. Filled black squares depict the DSC-determined tube-to-filament transition temperatures. Open red circles represent unentangled filaments, different tubes states: unentangled (UE-green triangles), partially entangled (PE-blue diamonds), and well-entangled (WE-pentagons). The full line  $T=88^{\circ}\text{C}$  separates tube from filament phases. The two dashed lines delimiting the 3 tube domains are  $c \sim e^{\frac{E_a}{k_B T}}$  dashed lines as explained in the text.

Besides their use to establish the phase diagram Fig. 3, LVE data can also be used to extract viscosities. Viscosity has widely been used as a marker of the different phases in EHUT.<sup>16</sup> In Fig. 4 we report the relative viscosities increment  $\eta_i = \eta_0^*/\eta_s - 1$  (the ratio of the zero-shear dynamic viscosity of EHUT  $\eta_0^*$  to the solvent viscosity  $\eta_s$ , minus one) as a function of a) concentration at different temperatures b) temperature at different concentrations.

Data for the filament solutions could be obtained but only over a rather limited concentration range as the viscosities were too low to be measured reliably. We observe that  $\eta_i$  conforms to  $\eta_i \sim c^2$  scaling, in agreement with findings from EHUT filament solutions in carbon tetrachloride<sup>31</sup> and somewhat stronger that the dilute scaling  $\eta_i \sim c/c^* \sim c^{1.25}$  expected for unentangled living supramolecular polymer solutions.<sup>5</sup> In the unentangled tube regime, the  $\eta_i$  values range again from 1 to 10, and the evolution is consistent with  $\eta_i \sim c^{1.25}$ . At higher concentrations in the entangled tubes regime, the data follow a  $\eta_i \sim c^{3.4}$  scaling, in excellent agreement with the Cates prediction and previous experimental results.<sup>11, 12</sup> We note that both power-law scaling exponents for  $\eta_i$  in the tube phase (1.25 and 3.4) are weaker than those recently reported for surfactant WLMs (1.7 and 5.0), which may suggest different  $L(c)$  for EHUT and WLMs.<sup>29</sup> A large jump of the viscosity at

the transition between unentangled and entangled regimes is clearly apparent in Fig. 4a at 25°C also clearly noticeable directly in the creep compliance (displayed in SI figS7). It suggests an almost discontinuous behavior of the viscosity when reaching the partially and well-entangled regimes. Interestingly, similar behavior can be observed in the WLM data.<sup>29</sup> Fig. 4b depicts the decrease of  $\eta_i$  with increasing temperature for different concentrations. The tube-to-filament transition (Fig.3) is marked by a change of viscosity, more apparent in the PE and WE regimes. The limited number of data points in the filament phase make it difficult to estimate an apparent activation energy. The larger change in  $\eta_i(T)$  appears to be at the entanglement transition (UE to PE), not unlike in the  $\eta_i(c)$  of Fig4a. In the WE regime, an apparent activation energy of about  $50 k_B T$  is measured. Typically,  $\eta_i$  is about 100 times higher at 25°C than at 80°C. This is in agreement to earlier findings<sup>14</sup> as depicted in Fig. S9. The point are too few to precisely evaluate the variation of the apparent activation energy with the concentration, but it seems limited in the WE regime. As to the T-dependence in the different domain, the living polymer model suggests a factor of 3 or so in the apparent activation energy, as  $\eta_i \sim L$  in the case of unentangled and  $L^{3.4}$  in entangled regime and the effect of Temperature on L is  $L \sim e^{\frac{E}{2 k_B T}}$ . The data are too few to clearly show this, but it would be interesting to check this effect.

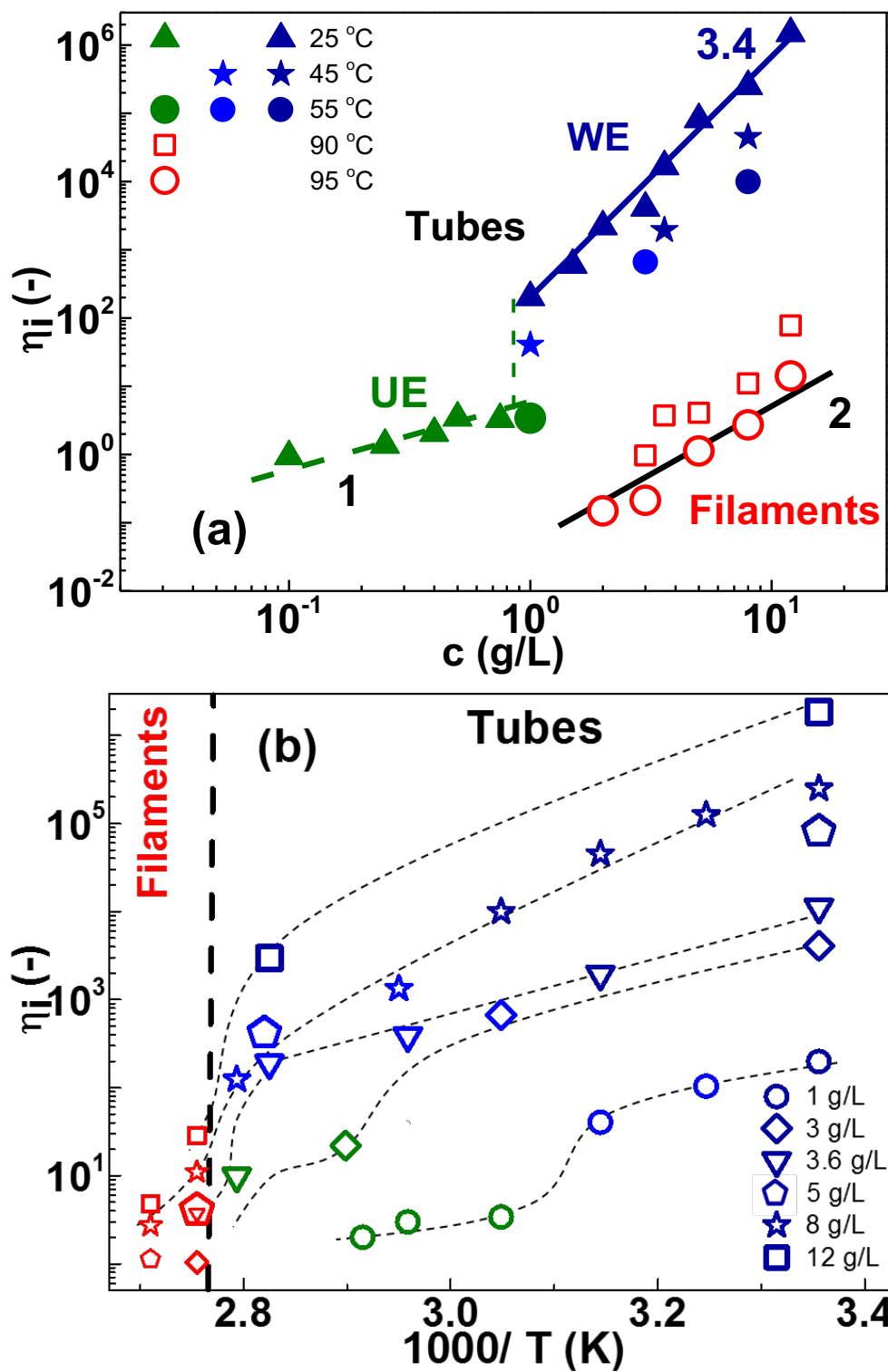


**Figure 5:** Relative viscosity increment ( $\eta_i$ ) of EHUT/dodecane solutions a) as a function of concentration at different temperatures with red symbols for filament phase, deep / light blue symbols for well / partially entangled (WE/PE) tube phase respectively, green symbols for unentangled (UE) tube phase. Temperature are indicated in the legend. b) as a function of temperature at different concentrations with same color coding and with concentrations given in legend.

## Conclusions

The evolution of rheology of the supramolecular EHUT solution in dodecane is reminiscent of the much studied WLM solutions<sup>5</sup>. Recently, the original Cates model was extended to account for constraint release effects (among others) and provides a way to describe the evolution of the LVE (and nonlinear) spectra over broad range of conditions.<sup>32</sup> A numerical approach has been developed along these lines and has been applied to WLMs over a broad range of parameters.<sup>33, 34</sup> In view of the presented complete dynamic phase diagram, it would be interesting to examine whether the method developed to analyze WLM rheology could be applied for EHUT and allow to retrieve values for average length, scission energy, persistence length, parameters that are difficult to obtain by other methods, in particular length and length distribution. Our results certainly further confirm the equivalence of EHUT supramolecular tubes and WLMs. However the scission mechanism in EHUT tubes is not fully elucidated, but is expected to be highly cooperative and possibly involving multiple steps. It nonetheless appears to be fast enough to allow equilibration and provide the expected channel for stress relaxation. Most of properties variation can be attributed to change of average length of the assembly, following the Cates living polymer theory. Generally, careful analysis of LVE is likely to provide insightful structural and dynamical information of supramolecular polymer assembly.

## Supporting information:

Schematic of DLS microrheology setup; DLS data; extracted rheological data; determination of different entangled regimes; specific viscosities ; alternative representation of the complete phase diagram.

## Acknowledgements

Partial support by the Greek Ministry of Education (INNOVATION program-AENAO) is gratefully acknowledged.

## REFERENCE

- [1] Greef T. F. A. De; Smulders M. M. J.; Wolffs M.; Schenning A. P. H. J.; Sijbesma R. P.; and Meijer E. W. Supramolecular Polymerization, *Chem. Rev.* **2009**, 109, 11, 5687–5754.
- [2] Krieg E.; Bastings M. M. C.; Besenius P.; Rybtchinski B. Supramolecular Polymers in Aqueous Media, *Chem. Rev.* **2016**, 116, 4, 2414–2477.

- [3] Matern J.; Dorca Y.; Sánchez L.; Fernández G.; Revising Complex Supramolecular Polymerization under Kinetic and Thermodynamic Control, *Angew. Chem.* **2019**, 58, 16730-16740.
- [4] Vereroudakis E.; & Vlassopoulos D. Tunable dynamic properties of hydrogen-bonded supramolecular assemblies in solution. *Prog. Pol. Sci.* **2021**, 112, 101321.
- [5] Cates M.; Reptation of living polymers: dynamics of entangled polymers in the presence of reversible chain-scission reactions, *Macromolecules*, **1987**, 20, 2289-2296.
- [6] Cates M.; Candau S. Statics and dynamics of worm-like surfactant micelles. *J. Phys.: Cond.Mat.* **1990**, 2, 6869.
- [7] Cates M.E.; & Fielding S.M. Rheology of giant micelles. *Adv. Phys.* **2006**, 55, 799-879.
- [8] Bouteiller L. Assembly via Hydrogen Bonds of Low Molar Mass Compounds into Supramolecular Polymers. Hydrogen Bonded Polymers. *Adv. Polym. Sci.* **2007**, 207, 79-112.
- [9] Lortie, F. ; Boileau, S. ; Bouteiller, L. ; Chassenieux, C. ; Demé, B. ; Ducouret, G. ; Jalabert, M. ; Lauprêtre, F.; Terech, P. Structural and rheological study of a bis-urea based reversible polymer in an apolar solvent. *Langmuir* **2002**, 18, 7218-7222.
- [10] Bellot, M.; Bouteiller, L. Thermodynamic description of bis-urea self-assembly: competition between two supramolecular polymers. *Langmuir* **2008**, 24, 14176-14182.
- [11] Van der Gucht, J.; Besseling N.; Knoben W.; Bouteiller L.; Stuart M. C. Brownian particles in supramolecular polymer solutions. *Physical Review E* **2003**, 67, 051106
- [12] Ducouret, G.; Chassenieux, C.; Martins, S.; Lequeux F.; Bouteiller, L. Rheological characterisation of bis-urea based viscoelastic solutions in an apolar solvent. *J. Colloid Interf. Sci.* **2007**, 310, 624-629.
- [13] Louhichi A.; Jacob A. R.; Bouteiller L.; Vlassopoulos D.; “Humidity affects the viscoelastic properties of supramolecular living polymers”, special issue on Associating polymers, *J. Rheol.* **2017**, 61, 1173-1182.
- [14] Knoben W.; Besseling N. A. M.; Stuart M. A. C. Rheology of a reversible supramolecular polymer studied by comparison of the effects of temperature and chain stoppers. *J. Chem. Phys.* **2007**, 126, 024907.
- [15] Bouteiller, L.; Colombani, O.; Lortie F.; & Terech P. Thickness transition of a rigid supramolecular polymer. *J. Am. Chem. Soc.* **2005**, 127, 8893–8898.
- [16] Isare B.; Pensec S.; Raynal M.; & Bouteiller L. Bisurea-based supramolecular polymers: From structure to properties. *Comptes Rendus Chim.* **2016**, 19, 148–156.
- [17] Pinault, T.; Isare B.; Bouteiller L. “Solvents with similar bulk properties induce distinct supramolecular architectures *ChemPhysChem.* **2006**, 7, 816-819.

- [18] Burger, N. A.; Mavromanolakis, A.; Meier, G.; P. Brocorens, R. Lazzaroni, Bouteiller, L.; Loppinet, B.; Vlassopoulos, D. Stabilization of supramolecular polymer phase at high pressures. *ACS Macro Let.* **2021**, 10, 321–326.
- [19] Massiera G.; Ramos L.; Ligoure C. Role of the size distribution in the elasticity of entangled living polymer solution. *Europhys. Lett.* **2002**, 57, 127-133.
- [20] Zou W.; Tan G.; Jiang H.; Vogt K.; Weaver M.; Koenig P.; Beaucage G.; Larson R.G. From well-entangled to partially-entangled wormlike micelles. *Soft Matter.* **2019**,15, 642-655
- [21] Shikata, T.;Nishida, T.; Isare, B.; Linares, M.; Lazzaroni, R.; Bouteiller, L. Structure and dynamics of a bisurea-based supramolecular polymer in n-dodecane. *J. Phys. Chem. B* **2008**, 112, 8459-8465.
- [22] Royall C. P.; Poon W. C. K.; Weeks E. R. “In search of hard spheres”, *Soft Matter.* **2013**, 9, 17-27.
- [23] Furst E. M. & T. M. Squires, *Microrheology*, Oxford University Press, NY 2017.
- [24] Waigh T.A. Advances in the microrheology of complex fluids. *Rep. Prog. Phys.* **2016**, 79 074601.
- [25] Squires T. M. & Mason T. G. Fluid Mechanics of Microrheology, *Ann. Rev. Fl. Mech.* **2010**, 42, 413-438.
- [26] Weese J. A regularization method for nonlinear ill-posed problems. *Comp. Phys. Com.* **1993**, 77,429-440.
- [27] Alvarenga, B. G.; Raynal, M.; Bouteiller, L.; Sabadini, E. Unexpected Solvent Influence on the Rheology of Supramolecular Polymers. *Macromolecules* **2017**, 50, 6631-6636.
- [28] Brocorens P.; Linares M.; Guyard-Duhayon C.; Guillot R.; Andrioletti B.; Suhr D.; Isare B.; Lazzaroni R.; Bouteiller L. Conformational Plasticity of Hydrogen Bonded Bis-urea Supramolecular Polymers, *J. Phys. Chem. B.* **2013**, 117, 5379–5386.
- [29] Tan, G.; Zou W.; Weaver M.; Larson R. G. Determining threadlike micelle lengths from rheometry. *J. Rheol.*, **2020**, 65, 59-71.
- [30] Rubinstein M.; & Colby R. *Polymer Physics*, Oxford University, New York, 2003.
- [31] Simic V.; Bouteiller L.; Jalabert M. Highly Cooperative Formation of Bis-Urea Based Supramolecular Polymers. *J. Am. Chem. Soc.* **2003**, 125, 13148-13154.
- [32] Peterson J.D. & Cates M.E. A full-chain tube-based constitutive model for living linear polymers, *J. Rheol.*, **2020**, 64, 1465.
- [33] Zou W.; & Larson R.G. A mesoscopic simulation method for predicting the rheology of semi-dilute wormlike micellar solutions. *J. Rheol.* **2013**, 58, 681-721.

[34] Sato T.; Moghadam S.; Tan G.; Larson R. G. A slip-spring simulation model for predicting linear and nonlinear rheology of entangled wormlike micellar solutions. *J. Rheol.* **2020**, 64, 1045-1061.